Critical behavior of quasi-two-dimensional semiconducting ferromagnet Cr_{2}Ge_{2}Te_{6}

Yu Liu (□□) and C. Petrovic

Phys. Rev. B **96**, 054406 — Published 3 August 2017

DOI: 10.1103/PhysRevB.96.054406

Critical behavior of quasi-two-dimensional semiconducting ferromagnet $Cr_2Ge_2Te_6$

Yu Liu (刘育) and C. Petrovic
Condensed Matter Physics and Materials Science Department, Brookhaven National Laboratory, Upton, New York 11973, USA
(Dated: July 17, 2017)

The critical properties of the single-crystalline semiconducting ferromagnet $Cr_2Ge_2Te_6$ were investigated by bulk dc magnetization around the paramagnetic to ferromagnetic phase transition. Critical exponents $\beta = 0.200\pm0.003$ with critical temperature $T_c = 62.65\pm0.07$ K and $\gamma = 1.28\pm0.03$ with $T_c = 62.75 \pm 0.06$ K are obtained by the Kouvel-Fisher method whereas $\delta = 7.96 \pm 0.01$ is obtained by the critical isotherm analysis at $T_c = 62.7$ K. These critical exponents obey the Widom scaling relation $\delta = 1 + \gamma/\beta$, indicating self-consistency of the obtained values. With these critical exponents the isotherm $M(H)$ curves below and above the critical temperatures collapse into two independent universal branches, obeying the single scaling equation $m = f_{\pm}(h)$, where m and h are renormalized magnetization and field, respectively. The determined exponents match well with those calculated from the results of renormalization group approach for a two-dimensional Ising system coupled with long-range interaction between spins decaying as $J(r) \approx r^{-(d+\sigma)}$ with $\sigma = 1.52$.

PACS numbers: 64.60.Ht,75.30.Kz,75.40.Cx

I. INTRODUCTION

Two-dimensional (2D) materials have recently stimulated significant attention not only for the emergence of novel properties but also for the potential applications.[1–5] In particular, layered intrinsically ferromagnetic (FM) semiconductors are of great interest since both ferromagnetism and semiconducting character are of interest for the next-generation spintronic devices.[6–11] $Cr_2X_2Te_6$ (X = Si, Ge) crystals belong to this class; they have an optical band gap of 0.4 eV for $Cr_2Si_2Te_6$ or 0.7 eV for $Cr_2Ge_2Te_6$,[5,10] and simultaneously, exhibit ferromagnetic ordering below the Curie temperature (T_c) of 32 K for $Cr_2Si_2Te_6$ or 61 K for $Cr_2Ge_2Te_6$, respectively.[10–15]

Considerable efforts have been devoted in order to shed light on the nature of ferromagnetism in bulk and monolayer $Cr_2X_2Te_6$.[16–20] Previous neutron scattering showed that bulk $Cr_2Si_2Te_6$ is a strongly anisotropic 2D Ising-like ferromagnet with a critical exponent $\beta = 0.17$ and a spin gap of $\sim$ 6 meV.[21] The critical behavior of $Cr_2Si_2Te_6$ investigated by bulk magnetization measurements further confirms the critical exponent $\beta = 0.170 \pm 0.008$, comparable to $\beta = 0.125$ for a 2D Ising model.[22] However, the recent neutron work on $Cr_2Si_2Te_6$ observed $\beta = 0.151$ and a very small spin gap of $\sim$ 0.075 meV.[23] Based on the spin wave analysis, the spins in $Cr_2Si_2Te_6$ are Heisenberg-like.[23] The spin wave theory also suggests that $Cr_2Ge_2Te_6$ is a nearly ideal 2D Heisenberg ferromagnet.[4] On the theoretical side, the Monte Carlo simulations based on a Heisenberg model predict the robust 2D ferromagnetism that exists in nano-sheets of a single $Cr_2X_2Te_6$ layer with $T_c \sim 35.7$ K for $Cr_2Si_2Te_6$ or $\sim$ 57.2 K for $Cr_2Ge_2Te_6$,[16] which can also be regarded as the theoretical prediction of corresponding bulk systems since only the nearest-neighbor (NN) exchange is considered. The predicted Curie temperatures are in good agreement with the experimental ones.[12,13] By further applying a moderate tensile strain, the 2D ferromagnetism is predicted theoretically to be largely enhanced with T_c increasing to $\sim$ 91.7 K for $Cr_2Si_2Te_6$ or $\sim$ 108.9 K for $Cr_2Ge_2Te_6$, respectively.[16] However, the Mermin-Wanger theorem states that long-range ferromagnetic order should not exist at non-zero temperature based on a 2D isotropic Heisenberg model,[24] with the exception of that the spins in the 2D system are constrained to only one direction, i.e., Ising-like spins.[25] Sivadas *et al.* claimed that when the second and third NN exchange interactions are considered, the monolayer $Cr_2Si_2Te_6$ is expected to be an antiferromagnet with a zigzag spin texture whereas $Cr_2Ge_2Te_6$ is still a ferromagnet with T_c of 106 K.[18] This is in contrast with the previous result where only the NN exchange interaction was considered.[16] It is also predicted that monolayer $Cr_2Si_2Te_6$ can be made ferromagnetic with T_c of 111 K when applying a moderate uniform in-plane tensile strain of $\sim$ 3%, which is experimentally feasible.[18] However, the recent scanning magneto-optic Kerr microscopy experiment on $Cr_2Ge_2Te_6$ shows that the T_c monotonically decrease with decreasing thickness, from bulk of about 68 K to a bilayer value of about 30 K,[4] which is in contrast to the theoretical prediction.

In order to clarify the magnetic behavior in few-layer samples and the possible applications of this material, it is necessary to establish the nature of the magnetism in the bulk. In this paper, we investigated the critical behavior of $Cr_2Ge_2Te_6$ by various techniques, such as modified Arrott plot, Kouvel-Fisher plot, and critical isotherm analysis. Our analysis indicate that the obtained critical exponents $\beta = 0.200 \pm 0.003$ ($T_c = 62.65 \pm 0.07$ K), $\gamma = 1.28\pm0.03$ ($T_c = 62.75\pm0.06$ K), and $\delta = 7.96\pm0.01$ ($T_c = 62.7$ K) are in good agreement with those calculated from the results of renormalization group approach for 2D Ising model coupled with long-range interaction between spins decaying as $J(r) \approx r^{-(d+\sigma)}$ with $\sigma = 1.52$.

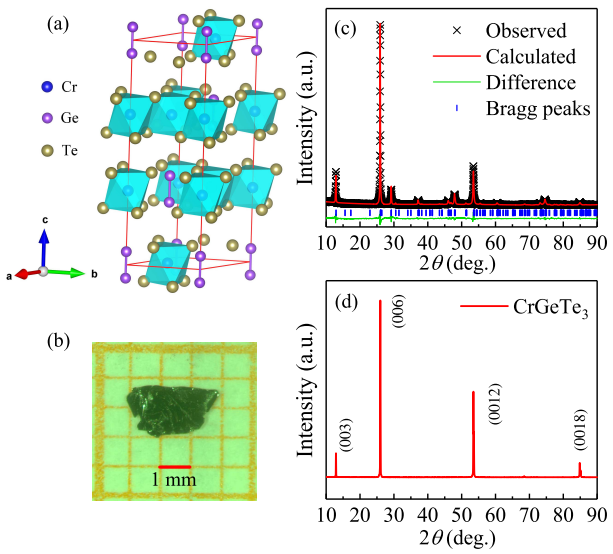

FIG. 1. (Color online). (a) Crystal structure of $Cr_2Ge_2Te_6$. (b) Image of a representative single-crystalline sample. (c) Powder x-ray diffraction (XRD) and (d) single-crystal XRD pattern of $Cr_2Ge_2Te_6$. The vertical tick marks represent Bragg reflections of the $R\bar{3}h$ space group.

II. EXPERIMENTAL DETAILS

High quality $Cr_2Ge_2Te_6$ single crystals were grown by the self-flux technique starting from an intimate mixture of pure elements Cr (99.95 %, Alfa Aesar) powder, Ge (99.999 %, Alfa Aesar) pieces, and Te (99.9999 %, Alfa Aesar) pieces with a molar ratio of 1 : 2 : 6. The starting materials were sealed in an evacuated quartz tube, which was heated to 1100 °C over 20 h, held at 1100 °C for 3 h, and then slowly cooled to 700 °C at a rate of 1 °C/h. X-ray diffraction (XRD) data were taken with Cu K_α (λ = 0.15418 nm) radiation of Rigaku Miniflex powder diffractometer. The element analysis was performed using an energy-dispersive x-ray spectroscopy (EDX) in a JEOL LSM-6500 scanning electron microscope. The magnetization was measured in a Quantum Design Magnetic Property Measurement System (MPMS-XL5). Isotherms were collected at an interval of 0.5 K around T_c. The applied magnetic field (H_a) has been corrected for the internal field as $H = H_a - NM$, where M is the measured magnetization and N is the demagnetization factor. The corrected H was used for the analysis of critical behavior.

III. RESULTS AND DISCUSSIONS

The bulk $Cr_2Ge_2Te_6$ is a well-known semiconducting ferromagnet, which was firstly synthesized by Carteaux *et al.*.[13] Figure 1(a) shows the crystal structure of $Cr_2Ge_2Te_6$. Each unit cell comprises of three $Cr_2Ge_2Te_6$ layers stacked in an ABC sequence along the c-axis. The

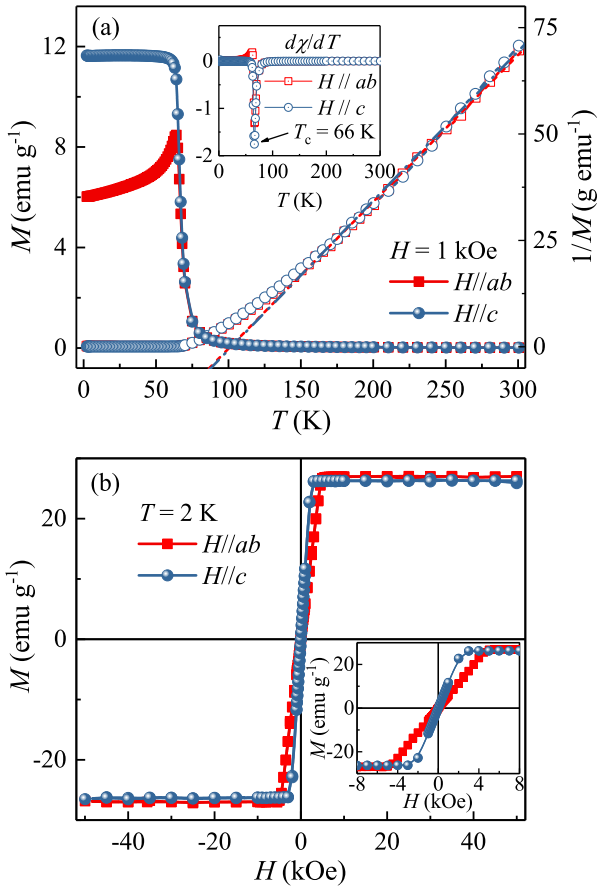

FIG. 2. (Color online). (a) Temperature dependence of magnetization for $Cr_2Ge_2Te_6$ measured in the magnetic field H = 1 kOe. Inset: the derivative magnetization dM/dT versus T. (b) Field dependence of magnetization for $Cr_2Ge_2Te_6$ measured at T = 2 K. Inset: the magnification of the low field region.

Cr ions are located at the centers of slightly distorted octahedra of Te atoms. The Ge pairs form Ge_2Te_6 ethane-like groups. The as-grown single crystals are plate-like, typically 3 to 4 mm in size, as shown in Fig. 1(b). Figure 1(c) presents the powder x-ray diffraction (XRD) pattern of $Cr_2Ge_2Te_6$, in which the observed peaks are well fitted with the $R\bar{3}h$ space group. The determined lattice parameters are $a = 6.826(2)$ Å and $c = 20.531(2)$ Å, which are very close to the values reported previously.[5,13] Furthermore, in the single crystal 2θ XRD scan [Fig. 1(d)], only $(00l)$ peaks are detected, indicating the crystal surface is normal to the c axis with the plate-shaped surface parallel to the ab-plane.

Figure 2(a) shows the temperature dependence of magnetization $M(T)$ measured under H = 1 kOe applied in the ab-plane and paralleling to c-axis, respectively. A clear paramagnetic (PM) to ferromagnetic (FM) transition is observed and the apparent anisotropy suggests that the crystallographic c-axis is the easy axis. As shown in the inset of Fig. 2(a), the critical temperature $T_c \approx 66$ K is roughly determined from the minimum

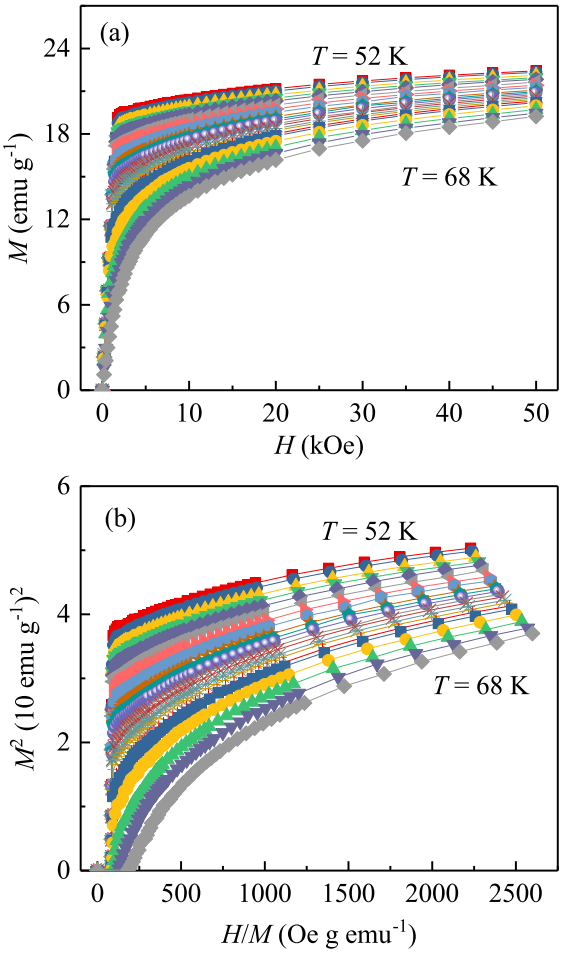

FIG. 3. (Color online). (a) Typical initial isothermal magnetization curves from T = 52 K to T = 68 K for $Cr_2Ge_2Te_6$. (b) Arrott plots of M^2 versus H/M around T_c for $Cr_2Ge_2Te_6$.

of the dM/dT curve, which is in good agreement with the value reported previously.[5,13] The temperature dependence of $1/M$ is also plotted in Fig. 2(a). A linear fit of the $1/M$ data in the temperature range of 150 to 300 K yields the Weiss temperature $\theta_{ab} \approx 108(1)$ K or $\theta_c \approx 113(2)$ K, which is nearly twice the value of T_c, indicating strong FM interaction. The effective moment μ_{eff} = 3.43(2) μ_B/Cr obtained from $H//ab$ data is identical to μ_{eff} = 3.41(5) μ_B/Cr from $H//c$ data, which is close to the the theoretical value expected for Cr^{3+} of 3.87 μ_B. Figure 2(b) displays the isothermal magnetization measured at T = 2 K. The saturation field $H_s \approx 3000$ Oe for $H//c$ is smaller than $H_s \approx 5000$ Oe for $H//ab$, confirming the easy axis is the c-axis. The saturation moment at T = 2 K is $M_s \approx 2.45(1)$ μ_B/Cr for $H//ab$ and $M_s \approx 2.39(1)$ μ_B/Cr for $H//c$, respectively, close to the expected value of 3 μ_B for Cr^{+3} with three unpaired spins. The inset of Fig. 2(b) shows the $M(H)$ in the low field region and the absence of coercive force (H_c) for $Cr_2Ge_2Te_6$. All these results are in good agreement with previous reports.[5,13]

The critical behavior of a second-order transition can be characterized in detail by a series of interrelated critical exponents.[26] In the vicinity of a second-order phase transition, the divergence of correlation length $\xi = \xi_0|(T - T_c)/T_c|^{-\nu}$ leads to universal scaling laws for the spontaneous magnetization M_s and the inverse initial magnetic susceptibility χ_0^{-1}. The spontaneous magnetization M_s below T_c, the inverse initial susceptibility χ_0^{-1} above T_c, and the measured magnetization $M(H)$ at T_c are characterized by a set of critical exponents β, γ, and δ. The mathematical definitions of these exponents from magnetization are:

$$M_s(T) = M_0(-\varepsilon)^{\beta}, \varepsilon < 0, T < T_c \tag{1}$$

$$\chi_0^{-1}(T) = (h_0/m_0)\varepsilon^{\gamma}, \varepsilon > 0, T > T_c \tag{2}$$

$$M = DH^{1/\delta}, \varepsilon = 0, T = T_c \tag{3}$$

where $\varepsilon = (T - T_c)/T_c$ is the reduced temperature, and M_0, h_0/m_0 and D are the critical amplitudes.[27] The magnetic equation of state is a relationship among the variables $M(H, \varepsilon)$, H, and T. Using scaling hypothesis this can be expressed as:

$$M(H, \varepsilon) = \varepsilon^{\beta} f_{\pm}(H/\varepsilon^{\beta+\gamma}) \tag{4}$$

where f_+ for $T > T_c$ and f_- for $T < T_c$, respectively, are the regular functions. In terms of renormalized magnetization $m \equiv \varepsilon^{-\beta} M(H, \varepsilon)$ and renormalized field $h \equiv \varepsilon^{-(\beta+\gamma)} H$, the Eq.(4) can be written as:

$$m = f_{\pm}(h) \tag{5}$$

it implies that for true scaling relations and right choice of β, γ, and δ values, scaled m and h will fall on two universal curves: one above T_c and another below T_c. This is an important criterion for the critical regime.

In order to clarify the nature of PM-FM transition in $Cr_2Ge_2Te_6$, we measured the isothermal $M(H)$ in the temperature range from T = 52 K to T = 68 K, as shown in Fig. 3(a). Generally, conventional method to determine the critical exponents and critical temperature involves the use of Arrott plot.[28] The Arrott plot assumes the critical exponents following the mean-field theory with β = 0.5 and γ = 1.0.[28] According to this method, isotherms plotted in the form of M^2 versus H/M constitute a set of parallel straight lines, and the isotherm at the critical temperature T_c should pass through the origin. At the same time, it directly gives $\chi_0^{-1}(T)$ and $M_s(T)$ as the intercepts on H/M axis and positive M^2 axis, respectively. Figure 3(b) shows the Arrott plot. All the curves in this plot show nonlinear behavior having downward curvature even in high fields. This suggests that the mean-field model is not valid for $Cr_2Ge_2Te_6$. According to the Banerjee's criterion,[29] one can estimate the order of the magnetic transition through the slope of the straight line: negative slope

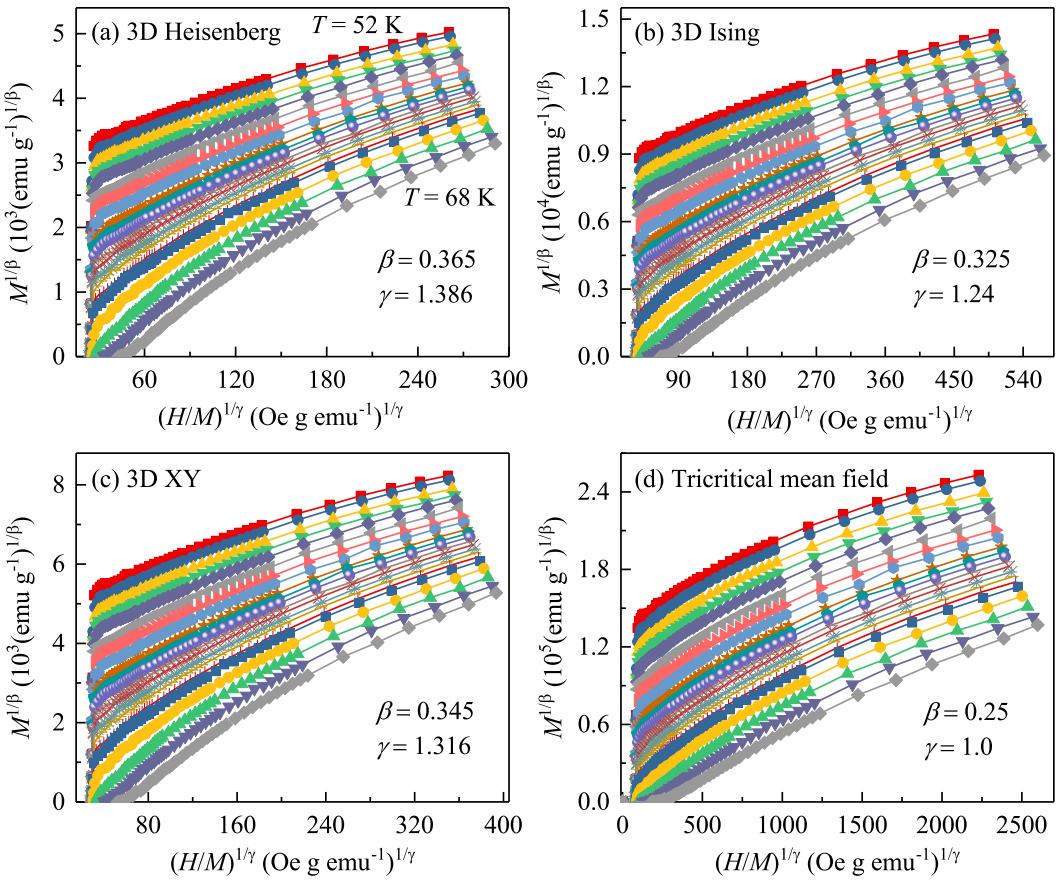

FIG. 4. (Color online). The isotherms plotted as $M^{1/\beta}$ versus $(H/M)^{1/\gamma}$ with (a) 3D-Heisenberg model; (b) 3D-Ising model; (c) 3D-XY model; and (d) Tricritical mean-field model.

TABLE I. Comparison of critical exponents of $Cr_2Ge_2Te_6$ and $Cr_2Si_2Te_6$ with different theoretical models.

Composition	Reference	Technique	β	γ	δ
$Cr_2Ge_2Te_6$	This work	Modified Arrott plot	0.196(3)	1.32(5)	7.73(15)
	This work	Kouvel-Fisher plot	0.200(3)	1.28(3)	7.40(5)
	This work	Critical isotherm			7.96(1)
$Cr_2Si_2Te_6$	22	Kouvel-Fisher plot	0.175(9)	1.562(9)	9.925(56)
2D Ising	30	Theory	0.125	1.75	15
Mean field	28	Theory	0.5	1.0	3.0
3D Heisenberg	28	Theory	0.365	1.386	4.8
3D XY	28	Theory	0.345	1.316	4.81
3D Ising	28	Theory	0.325	1.24	4.82
Tricritical mean field	29	Theory	0.25	1.0	5

corresponds to the first-order transition while positive corresponds to the second-order. Therefore, the concave downward curvature clearly indicates the PM-FM transition in $Cr_2Ge_2Te_6$ is a second-order one. We also examined other three-dimensional (3D) models, including 3D-Heisenberg ($\beta = 0.365$, $\gamma = 1.386$), 3D-XY ($\beta = 0.345$, $\gamma = 1.316$), 3D-Ising model ($\beta = 0.325$, $\gamma = 1.24$) and tricritical mean-field model ($\beta = 0.25$, $\gamma = 1.0$).[28,29] As shown in Fig.4, all these models failed to yield parallel straight lines, suggesting the breakdown of these 3D models.

Considering the strong two-dimensional (2D) characteristics in $Cr_2Ge_2Te_6$, we further analyze the isothermal data with 2D-Ising model ($\beta = 0.125$, $\gamma = 1.75$).[30] As shown in Fig. 5(a), a set of quasi-parallel straight lines are obtained. However, there is still no a single straight line that passes through origin, indicating that $Cr_2Ge_2Te_6$ can not be rigorously described by the 2D-

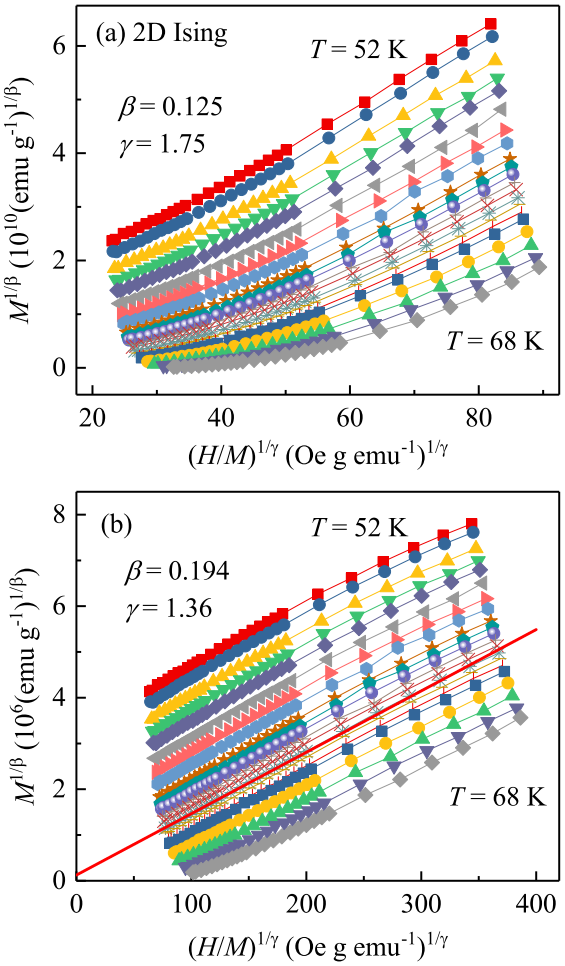

FIG. 5. (Color online). (a) 2D-Ising model plot of isotherms for $Cr_2Ge_2Te_6$. (b) Modified Arrott plot of $M^{1/\beta}$ versus $(H/M)^{1/\gamma}$ with $\beta = 0.194$ and $\gamma = 1.36$ for $Cr_2Ge_2Te_6$. The straight line is the linear fit of isotherm at $T = 62.5$ K.

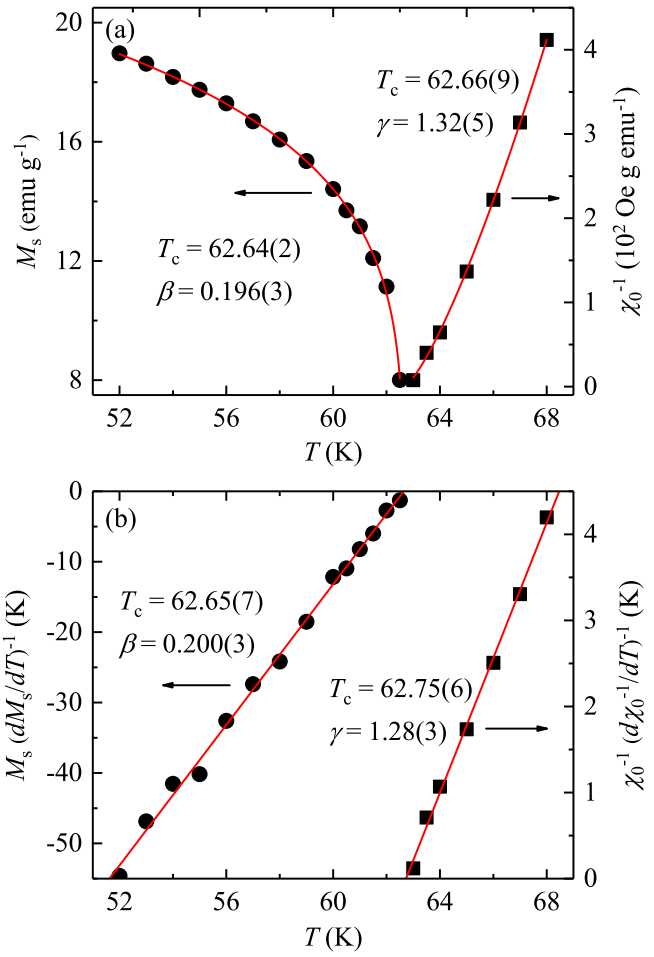

FIG. 6. (Color online). (a) Temperature dependence of the spontaneous magnetization M_s (left) and the inverse initial susceptibility χ_0^{-1} (right) with solid fitting curves for $Cr_2Ge_2Te_6$. (b) Kouvel-Fisher plots of $M_s(dM_s/dT)^{-1}$ (left) and $\chi_0^{-1}(d\chi_0^{-1}/dT)^{-1}$ (right) with solid fitting curves for $Cr_2Ge_2Te_6$.

Ising model. Therefore, a modified Arrott plot by a self-consistent method is further applied to determine T_c as well as the critical exponents β and γ.[31] The modified Arrott plot is given by the Arrot-Noaks equation of state:

$$(H/M)^{1/\gamma} = a\varepsilon + bM^{1/\beta} \tag{6}$$

where $\varepsilon = (T - T_c)/T_c$ is the reduced temperature, a and b are constants. To find out the proper values of β and γ, a rigorous iterative method has been used.[32] The starting values of $M_s(T)$ and $\chi_0^{-1}(T)$ were determined from the 2D-Ising model plot by the linear extrapolation from the high field region to the intercepts with the axis $M^{1/\beta}$ and $(H/M)^{1/\gamma}$, respectively. A new set of β and γ can be obtained by fitting data following the Eqs (1) and (2). Then the obtained new values of β and γ are used to reconstruct a new modified Arrott plot. This procedure was repeated until the values of β and γ are stable. By this method, the obtained critical exponents are hardly dependent on the initial parameters, which confirms these critical exponents are reliable and intrinsic. The final modified Arrot plots generated with the values $\beta = 0.194$ and $\gamma = 1.36$ are depicted in Fig. 5(b).

Figure 6(a) presents the final $M_s(T)$ and $\chi_0^{-1}(T)$ with the solid fitting curves. The critical exponents $\beta = 0.196(3)$ with $T_c = 62.64(2)$ K and $\gamma = 1.32(5)$ with $T_c = 62.66(9)$ K are obtained, which are very close to the values obtained from the modified Arrot plot in Fig. 5(b). Alternatively, the critical exponents can be determined by the Kouvel-Fisher (KF) method:[33]

$$\frac{M_s(T)}{dM_s(T)/dT} = \frac{T - T_c}{\beta} \tag{7}$$

$$\frac{\chi_0^{-1}(T)}{d\chi_0^{-1}(T)/dT} = \frac{T - T_c}{\gamma} \tag{8}$$

According to this method, $M_s(T)/[dM_s(T)/dT]$ and $\chi_0^{-1}(T)/[d\chi_0^{-1}(T)/dT]$ are as linear functions of temperature with slopes of $1/\beta$ and $1/\gamma$, respectively. As shown

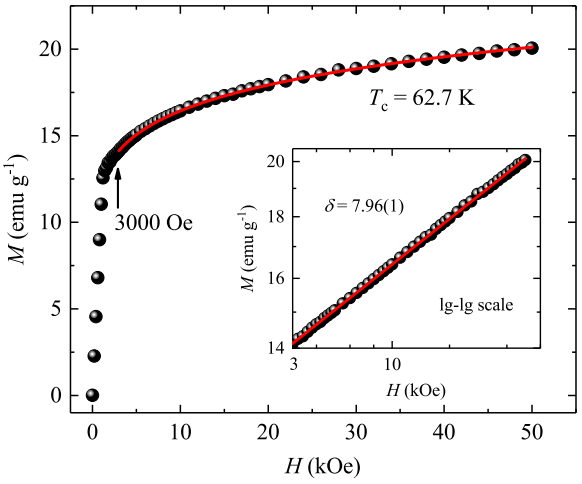

FIG. 7. (Color online). Isotherm M versus H plot collected at $T_c = 62.7$ K for $Cr_2Ge_2Te_6$. Inset: the same plot in log-log scale with a solid fitting curve.

in Fig. 6(b), the linear fits give $\beta = 0.200(3)$ with $T_c = 62.65(7)$ K and $\gamma = 1.28(3)$ with $T_c = 62.75(6)$ K, respectively.

The isothermal magnetization $M(H)$ at the critical temperature $T_c = 62.7$ K is shown in Fig. 7, with the inset plotted on a log-log scale. According to Eq. (3), the third critical exponent $\delta = 7.96(1)$ can be deduced. Furthermore, the exponent δ can also been calculated from Widom scaling relation according to which critical exponents β, γ, and δ are related in following way:

$$\delta = 1 + \frac{\gamma}{\beta} \tag{9}$$

Using the β and γ values determined from Modified Arrott plot and Kouvel-Fisher plot, we obtain $\delta = 7.73(15)$ and $\delta = 7.40(5)$, respectively, which are very close to the value obtained from critical isotherm analysis. Therefore, the critical exponents and T_c obtained in present study are self-consistent and an accurate estimate within experimental precision.

The reliability of the obtained critical exponents and T_c can also be verified by a scaling analysis. Following Eq. (5), scaled m versus scaled h has been plotted in Fig. 7(a), along with the same plot on lg-lg scale in the inset of Fig. 8(a). It is rather significant that all the data collapse into two separate branches: one below T_c and another above T_c. The reliability of the exponents and T_c has been further ensured with more rigorous method by plotting m^2 versus h/m, as shown in Fig. 8(b), where all data also fall on two independent branches. This clearly indicates that the interactions get properly renormalized in critical regime following scaling equation of state. In addition, the scaling equation of state takes another form:

$$\frac{H}{M^{\delta}} = k(\frac{\varepsilon}{H^{1/\beta}}) \tag{10}$$

where $k(x)$ is the scaling function. Based on Eq. (10), all experimental curves will collapse onto a single curve. The

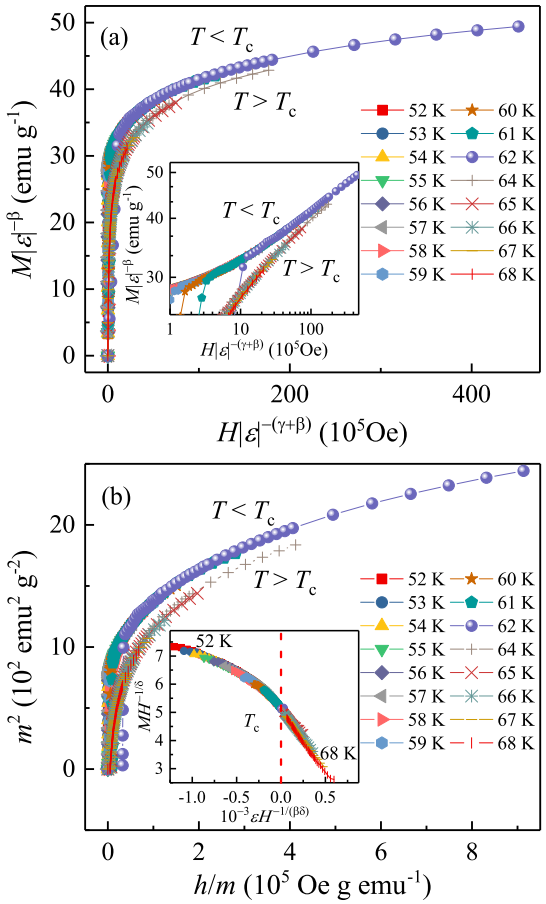

FIG. 8. (Color online). (a) Scaling plots of renormalized magnetization m versus renormalized field h below and above T_c for $Cr_2Ge_2Te_6$. Inset: the same plots in log-log scale. (b) the renormalized magnetization and field replotted in the form of m^2 versus h/m for $Cr_2Ge_2Te_6$. Inset: the rescaling of the $M(H)$ curves by $MH^{-1/\delta}$ versus $\varepsilon H^{-1/(\beta\delta)}$.

inset of Fig. 8(b) shows the $MH^{-1/\delta}$ versus $\varepsilon H^{-1/(\beta\delta)}$ for $Cr_2Ge_2Te_6$, where the experimental data collapse onto a single curve, and T_c locates at the zero point of the horizontal axis. The well-rescaled curves further confirm the reliability of the obtained critical exponents. All critical exponents derived from various methods are given in Table I along with the values of $Cr_2Si_2Te_6$ and the theoretically predicted values for different models. As we can see, the experimentally determined critical exponents β, γ, and δ are close to but show some deviation from the theoretical values of 2D-Ising model, which might be associated with non-negligible interlayer coupling and spin-lattice coupling in this material.[10,21] Compared to $Cr_2Si_2Te_6$ ($\beta = 0.175(9)$, $\gamma = 1.562(9)$), the critical exponents ($\beta = 0.200(3)$, $\gamma = 1.28(3)$) for $Cr_2Ge_2Te_6$ can be explained by larger Ge_2Te_6 octahedra and smaller van der Waals (VDW) gap that induced stronger interlayer coupling in $Cr_2Ge_2Te_6$.

Finally, we would like to discuss the nature as well as the range of interactions in $Cr_2Ge_2Te_6$. For a homo-

geneous magnet, the universality class of the magnetic phase transition depends on the exchange distance $J(r)$. Fisher *et al.* theoretically treated this kind of magnetic ordering as an attractive interaction of spins, where a renormalization group theory analysis suggests the interaction decays with distance r as:

$$J(r) \approx r^{-(d+\sigma)} \tag{11}$$

where d is the spatial dimensionality and σ is a positive constant.[34] According to this model, the range of the spin interaction is long or short depending on the $\sigma < 2$ or $\sigma > 2$, and it predicts the susceptibility exponent γ which has been calculated from renormalization group approach, as following:

$$\gamma = 1 + \frac{4}{d}(\frac{n+2}{n+8})\Delta\sigma + \frac{8(n+2)(n-4)}{d^2(n+8)^2} \times [1 + \frac{2G(\frac{d}{2})(7n+20)}{(n-4)(n+8)}]\Delta\sigma^2 \tag{12}$$

where $\Delta\sigma = (\sigma - \frac{d}{2})$ and $G(\frac{d}{2}) = 3 - \frac{1}{4}(\frac{d}{2})^2$. To find out the range of interaction (σ) as well as the dimensionality of both lattice (d) and spin (n) in this system we have followed the procedure similar to Ref. 35 where the parameter σ in above expression is adjusted for a particular values of $\{d : n\}$ so that it yields a value for γ close to that experimentally observed $\gamma = 1.28$. The so obtained σ is then used to calculate the remaining exponents from the following expressions: $\nu = \gamma/\sigma$, $\alpha = 2 - \nu d$, $\beta = (2 - \alpha - \gamma)/2$, and $\delta = 1 + \gamma/\beta$. This exercise is repeated for different set of $\{d : n\}$. We found that $\{d : n\} = \{2{:}1\}$ and $\sigma = 1.52$ give the exponents ($\beta = 0.256$, $\gamma = 1.617$, and $\delta = 7.32$) which are close to our experimentally observed values (Table I). This calculation suggests the spin interaction in $Cr_2Ge_2Te_6$ is of 2D Ising ($\{d : n\} = \{2{:}1\}$) type coupled with long-range ($\sigma = 1.52$) interaction.

IV. CONCLUSIONS

In summary, we have made a comprehensive study of the critical behavior at the PM-FM phase transition in the quasi-2D semiconducting ferromagnet $Cr_2Ge_2Te_6$. This transition is identified to be the second order in nature. The critical exponents β, γ, and δ estimated from various techniques match reasonably well and follow the scaling equation, confirming that the obtained exponents are unambiguous and intrinsic to the material. The determined exponents match well with those calculated from the results of renormalization group approach for a 2D Ising ($\{d : n\} = \{2{:}1\}$) system coupled with long-range interaction between spins decaying as $J(r) \approx r^{-(d+\sigma)}$ with $\sigma = 1.52$. *Note added.* Recently, we became aware that G. T. Lin *et al.*[36] also synthesized $Cr_2Ge_2Te_6$. Their conclusions regarding tricritical point ($\beta = 0.240(6)$, $\gamma = 1.000(5)$, $\delta = 5.070(6)$, $T_c = 67.9$ K) obtained by fitting in a different field range are not in conflict with our work ($\beta = 0.200(3)$, $\gamma = 1.28(3)$, $\delta = 7.96(1)$, $T_c = 62.7$ K) that are deduced from fitting in the field range from 5 kOe to 50 kOe for modified Arrott plot and from 3 kOe to 50 kOe for critical isotherm at $T_c = 62.7$ K, respectively.

ACKNOWLEDGEMENTS

We thank John Warren for help with SEM measurements. This work was supported by the U.S. DOE-BES, Division of Materials Science and Engineering, under Contract No. DE-SC0012704 (BNL)

[1] Q. H. Wang, K. Kalantar-Zadeh, A. Kis, J. N. Coleman, and M. S. Strano, Nat. Nanotechnol., **7**, 699 (2012).
[2] A. K. Geim, and I. V. Grigorieva, Nature, **499**, 419 (2013).
[3] S. Lebègue, T. Björkman, M. Klintenberg, R. M. Nieminen, and O. Eriksson, Phys. Rev. X, **3**, 031002 (2013).
[4] C. Gong, L. Li, Z. L. Li, H. W. Ji, A. Stern, Y. Xia, T. Cao, W. Bao, C. Z. Wang, Y. Wang, Z. Q. Qiu, R. J. Cava, S. G. Louie, J. Xia, and X. Zhang, Nature, doi:10.1038/nature22060 (2017).
[5] H. W. Ji, R. A. Stokes, L. D. Aegria, E. C. Blomberg, M. A. Tanatar, A. Reijnders, L. M. Schoop, T. Liang, R. Prozorov, K. S. Burch, N. P. Ong, J. R. Petta, and R. J. Cava, J. Appl. Phys., **114**, 114907 (2013).
[6] B. Sachs, T. O. Wehling, K. S. Novoselov, A. I. Lichtenstein, and M. I. Katsnelson, Rhys. Rev. B, **88**, 201402 (2013).
[7] I. Yamada, J. Phys. Soc. Jpn., **33**, 979 (1972).
[8] H. Kabbour, R. David, A. Pautrat, H. J. Koo, M. H. Whangbo, G. André, and O. Mentré, Angew. Chem., Int. Ed., **51**, 11745 (2012).
[9] M. A. McGuire, H. Dixit, V. R. Cooper, and B. C. Sales, Chem. Mater., **27**, 612 (2015).
[10] L. D. Casto, A. J. Clune, M. O. Yokosuk, J. L. Musfeldt, T. J. Williams, H. L. Zhuang, M. W. Lin, K. Xiao, R. G. Hennig, B. C. Sales, J. Q. Yan, and D. Mandrus, APL Mater., **3**, 041515 (2015).
[11] X. Zhang, Y. L. Zhao, Q. Song, S. Jia, J. Shi, and W. Han, Jpn. J. Appl. Phys., **55**, 033001 (2016).
[12] V. Carteaux, G. Ouvrard, J. C. Grenier, and Y. Laligant, J. Magn. Magn. Mater., **94**, 127 (1991).
[13] V. Carteaux, D. Brunet, G. Ouvrard, and G. André, J. Phys.: Condens. Matter, **7**, 69 (1995).
[14] G. Ouvrard, E. Sandre, and R. Brec, J. Solid State Chem., **73**, 27 (1988).
[15] B. Siberchicot, S. Jobic, V. Carteaux, P. Gressier, and G. Ouvrard, J. Phys. Chem., **100**, 5863 (1996).
[16] X. X. Li, and J. L. Yang, J. Mater. Chem. C, **2**, 7071 (2014).
[17] X. F. Chen, J. S. Qi, and D. N. Shi, Phys. Lett. A, **379**, 60 (2015).

[18] N. Sivadas, M. W. Daniels, R. H. Swendsen, S. Okamoto, and D. Xiao, Phys. Rev. B, **91**, 235425 (2015).
[19] J. P. Liu, S. Y. Park, K. F. Garrity, and D. Vanderbilt, Phys. Rev. Lett., **117**, 257201 (2016).
[20] M. W. Lin, H. L. Zhuang, J. Q. Yan, T. Z. Ward, A. A. Puretzky, C. M. Rouleau, Z. Gai, L. B. Liang, V. Meunier, B. G. Sumpter, P. Ganesh, P. R. C. Kent, D. B. Geohegan, D. G. Mandrus, and K. Xiao, J. Mater. Chem. C, **4**, 315 (2016).
[21] V. Carteaux, F. Moussa, and M. Spiesser, Europhys. Lett., **29**, 251 (1995).
[22] B. J. Liu, Y. M. Zou, L. Zhang, S. M. Zhou, Z. Wang, W. K. Wang, Z. Qu, and Y. H. Zhang, Sci. Rep., **6**, 33873 (2016).
[23] T. J. Williams, A. A. Aczel, M. D. Lumsden, S. E. Nagler, M. B. Stone, J. Q. Yan, and D. Mandrus, Phys. Rev. B, **92**, 144404 (2015).
[24] N. D. Mermin, and H. Wagner, Phys. Rev. Lett., **17**, 1133 (1966).
[25] H. L. Zhuang, Y. Xie, P. R. C. Kent, and P. Ganesh, Phys. Rev. B, **92**, 035407 (2015).
[26] H. E. Stanley, *Introduction to Phase Transitions and Critical Phenomena* (Oxford U. P., London and New York, 1971).
[27] M. E. Fisher, Rep. Prog. Phys., **30**, 615 (1967).
[28] A. Arrott, Phys. Rev. B, **108**, 1394 (1957).
[29] S. K. Banerjee, Phys. Lett., **12**, 16 (1964).
[30] J. C. LeGuillou, and J. Zinn-Justin, Phys. Rev. B, **21**, 3976 (1980).
[31] A. Arrott, and J. Noakes, Phys. Rev. Lett., **19**, 786 (1967).
[32] A. K. Pramanik, and A. Banerjee, Phys. Rev. B, **79**, 214426 (2009).
[33] J. S. Kouvel, and M. E. Fisher, Phys. Rev., **136**, A1626 (1964).
[34] M. E. Fisher, S. K. Ma, and B. G. Nickel, Phys. Rev. Lett., **29**, 917 (1972).
[35] S. F. Fischer, S. N. Kaul, and H. Kronmuller, Phys. Rev. B, **65**, 064443 (2002).
[36] G. T. Lin, H. L. Zhuang, X. Luo, B.J. Liu, F. C. Chen, J. Yan, Y. Sun, J. Zhou, W. J. Lu, P. Tong, Z. G. Sheng, Z. Qu, W. H. Song, X. B. Zhu, and Y. P. Sun, arXiv:1706.03239.